SECTION «ENGINEERING SCIENCES»

INVESTIGATION OF THE THERMODYNAMICS OF ALLOY PHASE TRANSFORMATION DURING THE FORMATION OF SHRINKAGE CAVITIES IN CASTINGS

Mykola Bosyi[1]

DOI: https://doi.org/10.30525/978-9934-26-715-4-50

Abstract. The contemporary evolution of the manufacturing and engineering sector demands a steady increase in the durability of metal components, alongside reductions in production costs and raw material use. Because casting is a preferred technique for creating complex components, the integrity of the final product relies heavily on stabilizing the thermophysical reactions within the mold. As liquid metal solidifies, it undergoes a natural reduction in specific volume. When the energy balance is uneven, this contraction generates shrinkage cavities and localized porosity. These imperfections compromise the casting's structural unity, introduce severe stress concentrations, and drastically reduce the overall strength of the components. *The purpose.* Research Objective. The primary goal of this study is to determine the underlying mechanisms governing how shrinkage cavities form and expand within castings. By establishing these patterns, this research intends to design scientifically sound manufacturing strategies that mitigate defects and refine the design of feeding systems. Key Research Tasks. To accomplish this objective, the following specific tasks will be addressed: Examine the theoretical frameworks surrounding the creation of thermal centers and the progression of the solidification front during non-isothermal alloy cooling. Analyze how the pouring temperature, mold material thermal conductivity, and overall casting shape collectively impact the location and volumetric size of shrinkage defects. Utilize three – dimensional computer simulations of the cooling process to pinpoint the exact regions where shrinkage defects are most likely to

[1] Senior Lecturer, Department of Materials Science and Foundry Production, Central Ukrainian National Technical University, Ukraine

© Mykola Bosyi

aggregate. Formulate actionable strategies to direct the solidification path by optimizing the positioning of risers and utilizing cooling elements to accelerate heat dissipation. This study investigates the phase transformation and volumetric contraction that occur as metallurgical alloys cool and solidify within a casting mold. Specifically, it focuses on how the thermal and geometric factors of the casting-mold system influence the shape, volume, and spatiotemporal development of the resulting shrinkage cavities. *Methodology.* The research objectives were addressed through a systematic analysis of casting processes. The theoretical framework utilizes foundational principles of fluid dynamics and heat transfer. For the simulation phase, specialized casting software was employed to implement numerical finite element analysis. To validate these model predictions, the study incorporated laboratory-scale melting, thermal analysis, and macrostructural evaluations of the cross-sections of the cast samples. *Results.* Research indicates that the rate of heat dissipation varies unevenly when pouring molten metal into sand-clay molds. During the first 15 to 30 seconds after the mold cavity is filled, a delicate solidified layer rapidly develops along the outer edges of the casting. Conversely, the advancement of the solidification front drops significantly – by a factor of 1.8 to 2.3 – in thick structural transitions and internal geometric corners when compared to flat sections. *Practical value:* A newly developed method for forecasting macrodefects caused by shrinkage enables engineers to optimize casting design without relying on excess metal. Implementing these guidelines in manufacturing boosts the yield of defect-free castings, cuts energy costs associated with remelting, and minimizes the need for final machining. *Novelty and originality:* This research clarifies how the speed of the solidification front interacts with shrinkage cavity shapes under fluctuating temperature gradients. Additionally, it introduces new quantitative metrics that define when an open shrinkage cavity shifts into internal porosity, based on the width of the alloy's two-phase zone.

INTRODUCTION

Relevance of the topic. Progress in the field of modern mechanical engineering is inextricably linked to the need to optimize material costs and simultaneously increase the structural strength of metal components. Among the variety of molding methods, casting confidently holds the leadership due

to the possibility of manufacturing parts of complex spatial configuration. At the same time, the final operational properties of cast products are determined by the nature of the passage of thermophysical phenomena during crystallization. A decrease in the specific volume of the melt during the phase transition from the liquid state to the solid state under conditions of power deficiency causes the appearance of local shrinkage cavities and sinks. The presence of such macrodefects destructively affects the integrity of the metal matrix, creates foci of increased internal stresses and reduces the resistance of structures to working loads. The use of outdated intuitive-empirical calculation schemes in the development of casting technology usually leads to either an artificial overestimation of metal content due to excessive dimensions of the profits, or the appearance of internal defects within the functional zones of the part. In view of this, a systematic study of the mechanisms and kinetics of shrinkage defect formation, taking into account the relationship between thermal and hydrodynamic parameters, appears to be an important scientific and applied task, the solution of which opens the way to controlled solidification and ensuring high density of the cast structure. Purpose and objectives of the study. The purpose of this scientific work is to identify the fundamental thermophysical patterns of the emergence and evolution of shrinkage cavities in cast blanks for the creation and implementation of progressive technological methods aimed at localization of defects and modernization of the design parameters of feed systems. To implement the outlined goal, the following tasks are envisaged: To analyze the theoretical aspects of the formation of local thermal centers and the kinetics of the phase transition boundary movement during uneven cooling of the melt. To determine the nature of the influence of thermal overheating of the liquid metal, thermophysical parameters of the shape and geometric features of the casting on the spatial arrangement and total capacity of shrinkage cavities. To apply three-dimensional digital modeling of solidification kinetics in order to detect potential locations of concentration of defects of shrinkage origin. The object of research is the physicochemical phenomena of crystallization and macroscopic volumetric changes of industrial alloys during their thermal cooling and transition to a solid state inside the casting cavity. The subject of research is the geometric configuration, capacity and kinetics of the development of shrinkage cavities, caused by the combined influence of temperature-

time conditions of solidification and design features of the "product-mold" system. Methodology and research methods. The solution of the identified scientific tasks was based on a systematic approach to the analysis of thermophysical phenomena in foundry production. The theoretical basis of the work is built on the classical provisions of hydrodynamics and heat transfer equations in continuous media. For applied research, the numerical method of finite elements was used, implemented using modern computer-aided engineering analysis (CAE) systems for foundry processes. The reliability of the theoretical results was confirmed by a series of control laboratory melts, fixation of cooling temperature curves (thermal analysis) and metallographic assessment of the macrostructure on cross-sections and sections of experimental samples. Scientific novelty of the obtained results. Scientific ideas about the nature of the interdependence between the rates of movement of the phase transition boundary and the geometric configuration of the shrinkage cavity under conditions of dynamic temperature gradient change have been deepened. New mathematically substantiated quantitative parameters have been formulated that describe the mechanism of the transition of a concentrated surface shell into internal microporosity as a function of the spatial extent of the crystallization interval of the alloy under study. Practical significance of the results obtained. An engineering algorithm for detecting zones of shrinkage macrocavities has been developed, which allows optimizing the parameters of the casting mold at the computer design stage and avoiding artificial overestimation of the dimensions of the profitable parts. The practical implementation of the proposed solutions in industrial conditions contributes to an increase in the utilization rate of liquid metal, minimizing the consumption of fuel and energy resources for remelting of scrap, as well as reducing the time and tool costs for the final machining of blanks.

1. Kinetics of the Formation of Shrinkage Cavities in a Cylindrical Casting Under Conditions of Comprehensive Cooling

We will analyze the peculiarities of the appearance of shrinkage defects in cylindrical casting during thermal exposure along the entire perimeter of the part.

The initial stage of crystallization of the casting is characterized by the formation of an outer hardened shell. The process of solidification of the

casting is initiated by the formation of a surface metal frame. The upper layers crystallize against the background of a constant fall of the melt mirror circulating in the interdendritic channels. If the rate of decrease in the volume of the liquid phase is inferior to the rate of crystallization of the upper zone, the liquid metal remains within the boundaries of the solidification zone. In such conditions, the formation of a single shrinking shell is excluded. Instead, the volume deficit is compensated by dispersed pores in the upper hardened crust. This defect of the macrostructure is easily fixed by the method of radiography on longitudinal templates [1; 2].

A concentrated shrinkage void is created at the moment when the liquid phase begins to decrease faster (or at the same rate) than the top layer of the crystallized metal grows. The air gap that appears between them gives rise to the defect.

The thickness of the solid phase on the surface of the casting is determined by the scale of the solidification zone and the ratio of the rates of crystallization from above and the drop of the melt level. Possessing high strength, this layer does not deform and does not fall when contact with the liquid phase is lost. As a result, there are no external shrinkage defects, and the sink itself is completely isolated inside the metal block. When, at the beginning of solidification, the liquid phase decreases faster than the solid layer grows in the upper part of the mold, a shrinkage cavity is formed until a stable surface crust appears. Under such conditions, the shell remains completely unprotected and open. When the rate of fall of the melt mirror is comparable to the rate of its crystallization from above, the upper hard layer manages to gain strength before the formation of the shrinkage cavity is completed. This leads to the separation of the shell by the so-called "bridge". For workpieces in the form of a cylinder with a height H, the current coordinate from the surface of the liquid phase to the base is usually denoted as y (Fig. 1).

Thus, knowing the dependence of y on time t, the formula for the rate of decrease in the liquid metal level can be written as follows:

$$\omega = \frac{d\left(H - y\right)}{d\tau} = -\frac{dy}{d\tau}, \quad (1)$$

or in dimensionless form:

$$W_l = -\frac{dy}{dF_0} \cdot \frac{1}{R}, \quad (2)$$

where $F_0 = a\tau/R^2$ – Fourier criterion;

$a = \lambda_m / C_m \gamma_m$ – coefficient of thermal conductivity of a solid metal crust;

λ_m, C_m, γ_m – coefficient of thermal conductivity, heat capacity and density of the hardened metal crust; R – casting radius.

The use of relative parameters (dimensionless time (F_0) and speed (W_l) allows you to compare modeling data for geometrically similar castings of different scales. The main requirement for such an analysis is the identity of the thermophysical properties of the alloy and the casting mold [3; 4].

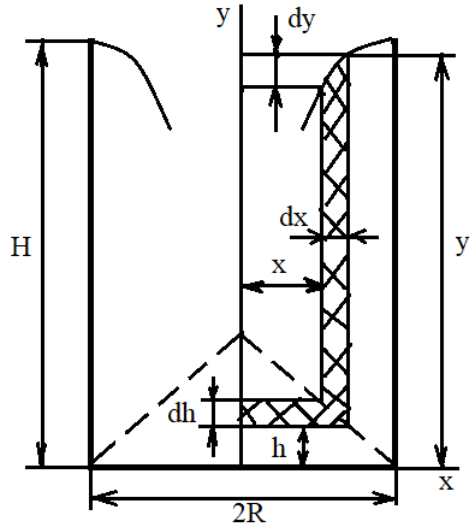


Figure 1. Calculation of the dynamics of the lowering of the metal melt level

A differential equation is used to calculate the drop in the liquid metal level.

$$\alpha_\upsilon \left[2\pi x (y - h) dx + \pi x_1^2 dh \right] = \pi x^2 dy , \qquad (3)$$

where α_υ – volume shrinkage coefficient.

In this equation, the left side reflects the amount of shrinkage of the elementary layers of the crystallized metal, while the right side determines the volume of the resulting shrinkage shell.

Assuming that the solidification of the metal through the upper surface of the olive occurs above the area, which in terms of transverse dimensions coincides with the lower one, but differs from it in thickness by (m_{sr}) times, and also taking into account the uniform speed of movement of the crystallization front from below and from the side, equation (3) takes the following form:

$$\pi\alpha_{\upsilon}\left[2xydx+\left(3+m_{sr}\right)x^2dx-2Rxdx\right]=\pi x^2dy, \quad (4)$$

where m_{sr} – the average ratio of the rate of phase transition of the melt in the upper part of the mold to the rate of its solidification in the bottom and side parts.

Let's solve this differential equation

$$\frac{dy}{dx}=\frac{2y+\left(3+m_{sr}\right)x-2R}{x}\alpha_{\upsilon}. \quad (5)$$

We rewrite it in another form

$$\frac{dy}{dx}=\frac{2y\alpha_{\upsilon}}{x}+\left[\left(3+m_{sr}\right)\alpha_{\upsilon}-\frac{2R}{3}\alpha_{\upsilon}\right]. \quad (6)$$

We exclude the last component and solve the equation, i.e.

$$\frac{dy_1}{dx}=\frac{2\alpha_{\upsilon}y_1}{x},\ y_1=C_1x^{2\alpha_{\upsilon}}. \quad (7)$$

The method of constant variation is used to find a solution to expression (7). The desired function is searched in the standard form for y, however, the C_1 coefficient is taken as a function.

Differentiating the expression (7), we get

$$y_1'=C_1x^{2\alpha_{\upsilon}}+C_1\cdot 2\alpha_{\upsilon}x^{2\varepsilon_{\upsilon}-1}. \quad (8)$$

Substituting parameters i into expression (6), we find

$$C_1'x^{2\alpha_{\upsilon}}+C_1\cdot 2\alpha_{\upsilon}x^{2\alpha_{\upsilon}-1}=C_1\frac{2\alpha_{\upsilon}}{x}x^{2\alpha_{\upsilon}}+\left(3+m_{sr}\right)\alpha_{\upsilon}-\frac{2R}{x}\alpha_{\upsilon}, \quad (9)$$

or

$$C_1'=\frac{\left(3+m_{sr}\right)}{x^{2\alpha_{\upsilon}}}\alpha_{\upsilon}-\frac{2R\alpha_{\upsilon}}{x^{2\alpha_{\upsilon}+1}}. \quad (10)$$

As a result of the integration of this expression, we get

$$C_1=-\left(3+m_{sr}\right)\alpha_{\upsilon}\frac{x^{-2\alpha_{\upsilon}+1}}{2\alpha_{\upsilon}-1}+\frac{2\alpha_{\upsilon}R}{2\alpha_{\upsilon}}x^{-2\alpha_{\upsilon}}+C. \quad (11)$$

Substituting C_1 into equation (7) we get

$$y = -\frac{(3+m_{sr})\alpha_\upsilon}{2\alpha_\upsilon - 1}x + R + x^{2\alpha_\upsilon}C. \quad (12)$$

The given initial parameters are used to calculate the integration constant: $x = R,\ y = H$

$$C = R^{1-2\alpha}\left[\frac{H}{R} + \frac{3+m_{sr}}{2\alpha_\upsilon - 1}\alpha_\upsilon - 1\right]. \quad (13)$$

Let's establish the dependence of the Fourier criterion on x

$$x = R - \varepsilon, \quad (14)$$

where e – thickness of the solid phase of the metal crust.

Below is the relationship describing the solidification of a cylindrical casting from a real melt:

$$F_0 - F_{0_1} = V_1'(\delta - \delta_1) + V_2'(\delta^2 - \delta_1^2) + V_3'(\delta^3 - \delta_1^3) + V_4' \ln \frac{1 + \frac{\delta Bi}{n_1}}{1 + \frac{\delta_1 Bi}{n_1}}, \quad (15)$$

where

$$V_1' = \frac{1}{Bi}\left(L + \frac{1}{n_1 + 1}\right) + \frac{n_1}{(n_1+1)(n_1+2)Bi^2};$$

$$V_2' = \frac{1}{2n_1}\left(L + \frac{1}{n_1+1}\right) - \frac{1}{2Bi}\left[L + \frac{1}{(n_1+1)(n_1+2)}\right];$$

$$V_3' = -\frac{1}{3n_1}\left[L + \frac{2}{(n_1+1)(n_1+2)}\right];$$

$$V_4' = -\frac{n_1}{(n_1+1)Bi^2}\left[1 + \frac{n_1}{(n_1+2)Bi}\right],$$

n_1 – coefficient, which depends on the temperature distribution across the section of the hardened metal crust;

Bi – the Biot criterion, which reflects the specific rate of heat exchange between the casting and the form;

$L = \dfrac{\rho + C_1 \Delta t_{cr}}{C_{ef}\left(t_{cr} - t_{m.s.}\right)}$ – dimensionless heat of crystallization;

C_{ef} – effective heat capacity of the system within the temperature range of solidification.

$$C_{ef} = C_1 + \frac{\rho}{\Delta t_{cr}},$$

C_1 – the actual specific heat capacity of the alloy;

ρ – the actual specific heat of the crystallization process of the alloy;

$\dfrac{\rho}{\Delta t_{cr}}$ – an imaginary increase in the heat capacity of the casting alloy in the crystallization temperature range, due to the generation of the latent heat of the phase transition;

t_{cr} – the temperature that characterizes the crystallization of the alloy;

$t_{surface}$ – the temperature of the cooling medium (form surface);

$\delta = \varepsilon / R$ – the relative thickness of the hardened crust of the metal;

$\delta_1 = \varepsilon_1 / R$ – Initial relative thickness of the formed hard metal layer;

$Fo = a\tau / R$ – the Fourier criterion characterizing the temporal development of the process;

$Fo_1 = a\tau_1 / R$ – the Fourier criterion corresponding to the beginning of the process.

Taking the moment of the beginning of crystallization as the reference point of time $\delta_1 = 0$ and setting the parameter n = 1 (which indicates a linear temperature profile along the thickness of the solidified layer), on the basis of dependence (15) we find:

$$F_0 = V_1\delta + V_2\delta^2 + V_3\delta^3 + V_4 \ln\left(1 + \delta Bi\right), \tag{16}$$

where $V_1' = \dfrac{1}{Bi}\left(L + 0{,}5\right) + \dfrac{1}{6Bi^2}$;

$$V_2' = 0{,}5\left(L + 0{,}5\right) - \frac{1}{2Bi}\left(L + \frac{1}{6}\right);$$

$$V_3' = -\frac{1}{3}\left(L + \frac{1}{3}\right);$$

$$V_4' = -\frac{0{,}5}{Bi^2}\left(1 + \frac{1}{3Bi}\right).$$

The calculated term d^3 is neglected for simplicity. The resulting error will be corrected at the next stage.

Expanding the left part of expression (16) into a Taylor series and limiting ourselves to the first two terms, after elementary transformations we find:

$$A\delta^2 + B\delta - Fo = 0\,, \tag{17}$$

where $A = V_2 - V_4\, Bi^2/2$; $B = V_1 + V_4 Bi$.

$$\delta = \frac{-B + \sqrt{B^2 + 4AFo}}{2A} \tag{18}$$

$$\text{or } \varepsilon = -\frac{BR}{2A} + \frac{R}{2A}\sqrt{B^2 + 4AFo}\,. \tag{19}$$

The found value of the thickness of the solidified metal made it possible to reveal the dependence of the height of the liquid phase on the Fourier criterion with the help of expressions (12) and (14).

$$y = -\frac{(3 + m_{sr})}{2\alpha_\upsilon - 1}\alpha_\upsilon\left(R + \frac{BR}{2A} - \frac{R}{2A}\sqrt{B^2 + 4AFo}\right) +$$

$$+R + \left(R + \frac{BR}{2A} - \frac{R}{2A}\sqrt{B^2 + 4AFo}\right)^{2\alpha_\upsilon} C. \tag{20}$$

Expression (20) is based on the dimensionless rate of lowering of the melt level for castings of cylindrical shape.

$$W_l = -\frac{dy}{dFo}\cdot\frac{1}{R} = \frac{\alpha_\upsilon}{\sqrt{B^2 + 4AFo}}\left\{\frac{3 + m_{sr}}{1\text{-}2\alpha_\upsilon} + \right.$$

$$\left. +2\left[\frac{H}{R} + \alpha_\upsilon\frac{3 + m_{sr}}{2\alpha_\upsilon - 1} - 1\right]\left(1 + \frac{B}{2A} - \frac{1}{2A}\sqrt{B^2 + 4AFo}\right)^{2\alpha_\upsilon - 1}\right\}. \tag{21}$$

Analysis of dependence (21) confirms that the rate of fall of the liquid phase level increases with an increase in thermal cooling, the shrinkage coefficient, and the relative height of the casting. The parameter of the average ratio of top and side solidification rates remains insignificant for geometry with an aspect ratio close to unity [5; 6].

The condition under which a shrinkage shell begins to form in the casting, where u – the rate of crystallization of the casting from above, is expressed as follows,

$$\frac{u}{W_l} \le 1 . \qquad (22)$$

For castings with a flat closed top, the dimensionless rate of crystallization can be determined from the following expression [5; 6]:

$$\mathrm{Fo} - \mathrm{Fo}_1 = C_1'\left(\delta_п - \delta_{п1}\right) + C_2'\left(\delta_п^2 - \delta_{п1}^2\right) + C_4' \ln \frac{1 + \frac{\delta_п Bi}{n_1}}{1 + \frac{\delta_{п1} Bi}{n_1}} , \qquad (23)$$

where $d_п$ – the relative depth of solidification of the metal crust;

$\delta_{п1}$ – initial relative thickness of the formed layer of solidified metal;

$$C_1' = \frac{1}{Bi}\left(L + \frac{1}{n_1 + 1}\right);$$

$$C_2' = \frac{1}{2n_1}\left(L + \frac{1}{n_1 + 1}\right);$$

$$C_3' = -\frac{n_1}{n_1 + 1} \cdot \frac{1}{Bi^2} .$$

The values of the others indicated have not changed (15).

Assuming that the superheat of the alloy is zero, i.e., $\tau_1 = Fo_1 = \delta_{n_1} = 0$ the time to fill the mold is infinitesimally small, and $n_1 = 1$, the mathematical expression (23) takes the following form:

$$Fo = C_1\delta_п + C_2\delta_п^2 + C_3 \ln\left(1 + \delta_п Bi\right), \qquad (24)$$

where $C_1 = \frac{1}{Bi}\left(L + 0{,}5\right)$; $C_2 = 0{,}5\left(L + 0{,}5\right)$; $C_3 = -0{,}5\frac{1}{Bi^2}$.

To find $d_п$ we will replace its natural logarithm with its linear approximation, as a result of which the desired ratio will take the form

$$D\delta_п^2 + D\delta_п - Fo = 0 , \qquad (25)$$

where $D = C_2 - C_3 Bi^2 / 2$; $E = C_1 + C_3 Bi$.

From expression (25), we find $d_п$

$$\delta_{\text{п}} = -\frac{E}{2D} + \frac{1}{2D}\sqrt{E^2 + 4DFo}\,. \tag{26}$$

The application of this mathematical expression allows you to calculate the dimensionless rate of crystallization of the upper part of the casting.

$$u = \frac{d\delta_{\text{п}}}{dFo} = \frac{1}{\sqrt{E^2 + 4DFo}}\,. \tag{27}$$

After substituting expressions (27) and (21) into the ratio (22) and the fixed value $m_{SR} = 1$, the calculation for castings closed from above takes the following form:

$$\frac{1}{\sqrt{E^2 + 4DFo}} = \frac{\alpha_{\upsilon}}{\sqrt{B^2 + 4AFo}} + \frac{1}{2D}\sqrt{E^2 + 4DFo}$$

$$\frac{1}{\sqrt{E^2 + 4DFo}} = \frac{\alpha_{\upsilon}}{\sqrt{B^2 + 4AFo}}\left\{\frac{4}{1\text{-}2a_{\upsilon}} + 2\left[\frac{H}{R} + \frac{4\alpha_{\upsilon}}{2\alpha_{\upsilon} - 1} - 1\right]\times\right.$$

$$\left.\times\left(1 + \frac{B}{2A} - \frac{1}{2A}\sqrt{B^2 + 4AFo}\right)^{2\alpha_{\upsilon}-1}\right\}. \tag{28}$$

For castings with a closed top, the initial stage of the formation of the concentration shrinkage sink is determined by the value of the Fourier criterion from expression (28). If at the same time it is known where exactly the border of spillage passes at a given moment, it is possible to calculate the geometric dimensions of the upper base of the sink [7; 8].

When manufacturing open castings, which are often used in industry, the reference point for the formation of a localized shrinkage shell is found using the equation:

$$\frac{u_1}{W_l} = \frac{mW_{solid}}{W_l} \le 1\,, \tag{29}$$

where u_1 – dimensionless speed of solidification of the upper part of the casting;

W_{solid} – dimensionless speed of solidification of the casting from the side;

m – existing ratio of the intensity of cooling of the casting in the upper and lateral directions.

The use of the averaged ratio of the solidification rates of the upper and side parts of the casting in the numerator of expression (29) is unacceptable,

contrary to the approach used in determining the rate of decrease of the melt level. Since the parameter directly determines the intensity of solidification of the metal from above, it must be calculated individually for each time interval.

The calculation of the solidification rate of the lateral surface of the casting is performed according to expression (18)

$$W_{\text{solid}} = \frac{d\delta}{dF_0} = \frac{1}{\sqrt{B^2 + 4AFo}}. \quad (30)$$

In order to calculate the ratio between the solidification rates of the casting in the upper and side parts, we will analyze the heat transfer process by the surface cooling in the open air. This heat exchange has a combined nature and includes convection (contact) and radiation. At the same time, the total density of the heat flow from the side of cooling is calculated as:

$$q = q_{\text{s. c. air}} + q_{\text{tr.r.}}, \quad (31)$$

где $q_{\text{s. c. air}}$ – intensity of heat exchange arising as a result of contact of the surface with the cooling air stream;

$q_{tr.r.}$ – specific heat transfer by radiation from the cooling surface.

Heat transfer during direct contact between media obeys the Newton-Richmann law

$$q_{\text{s. c. air}} = \alpha^T_{\text{s. c. air}} \left(t_{\text{s.}} - t^{\text{v}}_{\text{e}}\right), \quad (32)$$

where $\alpha^T_{\text{s. c. air}}$ – coefficient of contact heat exchange;

t_{s} – temperature indicator of the cooling surface;

t^{v}_{e} – the temperature of the casting cooling medium.

$$q_{\text{tr.r}} = \alpha^T_{\text{tr.r}} \left(t_{\text{s}} - t^{\text{v}}_{\text{e}}\right), \quad (33)$$

where $\alpha^T_{\text{tr.r}}$ – radiation heat transfer coefficient.

$$\alpha^T_{\text{tr.r}} = \frac{C_0 \left(\frac{T_{\text{s}}}{100}\right)^4}{t_{\text{s}} - t^{\text{v}}_{\text{e}}}, \quad (34)$$

where T_{s} – the temperature of the cooling surface layer, measured in Kelvin; C_0 – emissivity of a real body.

In this case, the total density of the heat flux emitted by the surface is

$$q = \alpha^T \left(t_s - t_e^v \right), \tag{35}$$

where $\alpha^T = \alpha_c^T + \alpha_{tr.r}^T -$ overall heat transfer coefficient.

Calculation of the heat transfer coefficient during contact was performed according to the method proposed in [7; 8].

The value is determined by the physical characteristics of the cooling medium and the intensity of its natural movement.

The product of the Grashof Gr and Prandtl criteria allows one to quantitatively assess the physical properties of the environment and the intensity of natural convection. Let's calculate this value for air acting as a cooling agent

$$Gr = \beta_c \frac{gd^3}{\nu^2} \Delta t, \tag{36}$$

where β_c – index of thermal expansion of air, which determines the change in its volume when heated; g – acceleration of gravity; ν_c– kinematic viscosity of air, $\nu_c = \eta_c / \gamma_c$; η_c – parameter of internal resistance (flowability) of the medium; γ_c – specific weight of air; d – defining linear dimension. For castings of a cylindrical shape, it is the outer diameter; $\Delta t = t_s - t_e^v -$ temperature pressure.

The calculation can be performed for an ambient temperature of 20 °C. Substitution of tabular physical parameters of air for given conditions in formula (36) gives: (β_c =0,00367oC^{-1}; γ_c = 0,061205 г/см^3; η_c =0,01842 г/см·с), we will receive

$$Gr = 1,5 \cdot 10^{-6} d^3 \Delta t. \tag{37}$$

To find the Prandtl criterion, we use the expression

$$Pr = \frac{\nu_c}{a_c}, \tag{38}$$

where $a_c = \lambda_c / \left(C_c ë_c \right) -$ thermal conductivity of air.

After substituting the thermophysical characteristics of the medium ν_c, λ_c,C_c, γ_c into formula (38), we obtain:

As a result of substituting the values in expression (38), we have:

$$Pr = 6,3 \cdot 10^6. \tag{39}$$

Multiplying the left and right parts of equations (37) and (39) by terms allows us to obtain the desired expression:

$$GrPr = 9,5 d^3 \Delta t. \tag{40}$$

For a preliminary assessment of this product, let's take the temperature pressure Δt =1000 °C. In this case, when the characteristic size of the body varies from 0.1 to 1.0 m, the calculated value of the criterion $GrPr$ changes in the range from 10 to 10^4. In particular $Gr \cdot Pr > 5 \cdot 10^2$, under the condition that the corresponding determining size is equal to $d > 0,4$ m, the convective heat transfer coefficient will be:

$$\alpha_c^T = V_1^T \frac{\Delta t^{0,25}}{d^{0,25}}, \quad (41)$$

where $V_1^T -$ is the coefficient, the value of which depends on the determining temperature. The latter is calculated using the following formula:

$$t = \frac{t_s + t_e^v}{2}. \quad (42)$$

At values $10^{-3} < GrPr < 5 \cdot 10^2$, that correspond to a change in the determining size ot $0,005 < d < 0,4$ m, the convective heat transfer coefficient is found from the expression:

$$\alpha_c^T = V_2^T \frac{\Delta t^{0,125}}{d^{0,625}}, \quad (43)$$

where $V_2^T -$ is a parameter depending on the determining temperature.

The values V_1^T, V_2^T of the coefficients are used in calculation dependences (41) and (43) for practical engineering calculations. Based on equations (34), (35), (41) and (43), we will find the total heat transfer coefficient as a function of the geometric dimensions and the temperature of the cooled surface. As the initial conditions, we will take the temperature of the surrounding air equal to 20 °C, and the object of research is steel and cast iron castings. The degree of blackness of these materials is assumed to be the same, while the radiation coefficient of an absolutely black body (taking into account the given emissivity) is C_0 = 18.83 kJ/m^2·h K^4 [7-9].

The results of the calculations show that the value of the coefficient of heat transfer by contact for surfaces of different sizes of castings made of steel and cast iron is very small and has almost no effect on the total coefficient of heat transfer. The relative difference in the results increases

as the surface temperature decreases. But even at 400°C, this difference is still quite small. All this gives the basis for using in further calculations the average values of the total heat transfer coefficient for surfaces of different sizes (Table 1):

Table 1

Calculated data of the total heat transfer coefficient for surfaces of various sizes

t_{air}, °C	1500	1400	1300	1200	1100	1000	900	800	700	400
α_{sr}^{T}, $\frac{kJ}{m^2 \cdot h. \, ^\circ C}$	1272	1125	920	765	635	518	418	335	263	115

Finding the total specific heat flux according to formula (31) requires the presence of a time dependence of the temperature of the cooling surface. The desired regularity was established experimentally during the study of cylindrical castings made of gray iron of different chemical composition (height of samples – 400 mm, diameter – 300 mm), made in dry sand-clay molds. The measurement of temperature parameters was performed at the central point of the open surface of the casting with the help of a platinum-platinum rhodium immersion thermocouple, and the time intervals were recorded using a stopwatch (Fig. 2).

Let us assume that the coefficient *m* is expressed as the ratio of the heat flux densities from the top and side surfaces of the casting.

$$m = \frac{q_b}{q_\delta} = \frac{\alpha_{sr}^{T}\left(t_s - t_e^{v}\right)}{b_f \theta_p}\sqrt{\tau}, \tag{44}$$

where $\theta_p = t_{s.} - t_{init}$ – is the surface temperature of the mold, reduced to the initial zero (t_{init} = 20 °C);

$b_f = \frac{\sqrt{a}\rho\gamma_m}{\sqrt{Fo_3}\left(t_{cr} - t_{init}t\right)}$ – heat accumulation coefficient of the mold;

Fo_3 – the Fourier criterion, at the moment of complete solidification of the casting; t – duration (or time) of the hardening process.

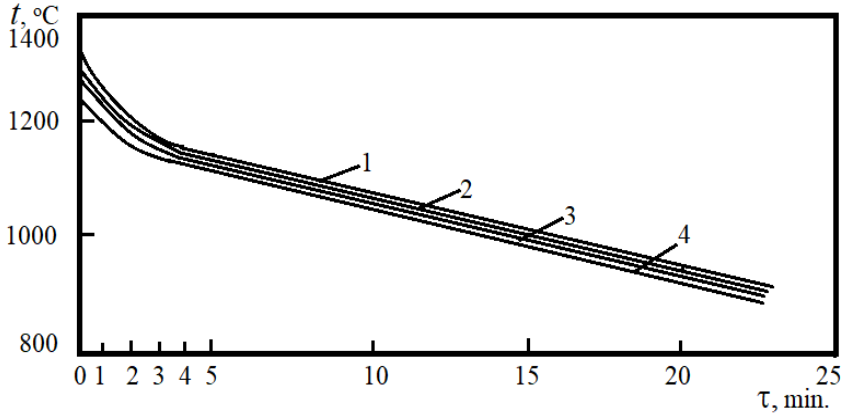


Figure 2. The process of air cooling of the surface of a cylindrical casting made of gray cast iron: 1,2,3,4 – cast iron series with a carbon equivalent, respectively: 3,7; 3.8; 4.0; 4.3

Based on the assumption $t_{cr} = \left(t_{liq} + t_{solid}\right)/2$, the value of the Fourier criterion, corresponding to the completion of solidification, is found on the graphs of the kinetics of crystallization of cast iron cylindrical castings in raw sand molds [8; 9], presented in Fig. 3.

According to data [8; 9], the temperature, for example, for iron castings is taken to be equal to 900 °C. Based on the selected value for example α_{sr}^{T}, on the known temperature of the upper open surface of the casting, the parameter *m* t is calculated for cylindrical castings from eutectic cast iron depending on the duration of the crystallization process. The calculation results are shown in Fig. 4. It can be seen from the graphs that the ratio of the solidification rates of the casting in the upper and lateral directions initially increases from zero, but then decreases, forming an extremum (maximum). The presence of the maximum is caused by a sharp drop in the specific heat flux from the open surface of the casting as it cools.

The results of the calculations show that the values of the ratio of the solidification rates in the upper and lateral directions for castings made of cast iron of different compositions differ slightly. Consequently, with sufficient accuracy for engineering calculations, it is possible to use those shown in Fig. 4 values of coefficient *m* for castings from any grades of cast iron.

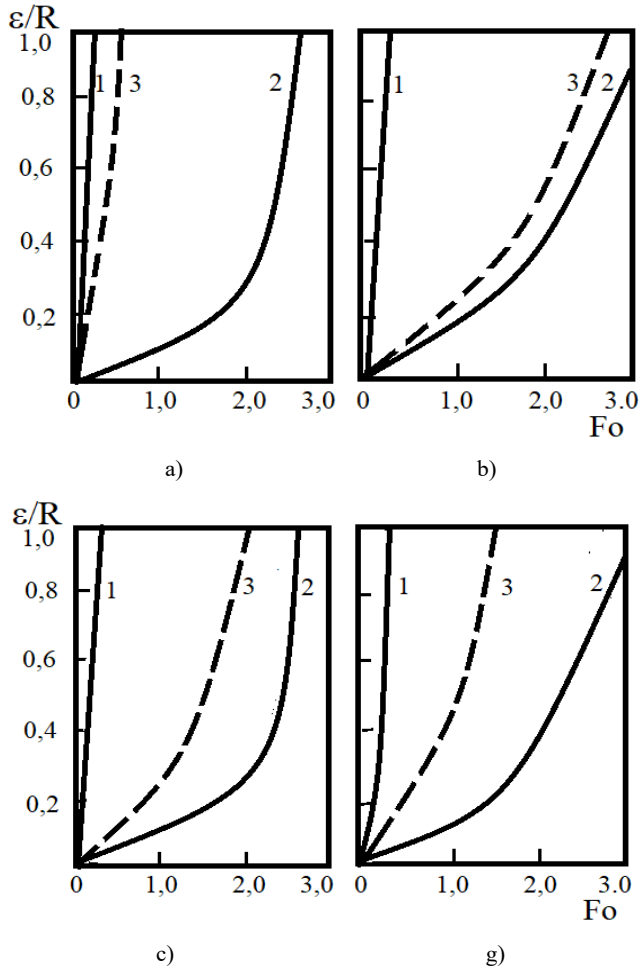


Figure 3. The process of solidification of cylindrical iron castings in raw sand form: magnesium cast iron castings: a – pre-eutectic, b – gray eutectic cast iron; c – from magnesium cast iron of eutectic composition; g - from magnesium cast iron of a eutectic composition; 1 – front of the beginning of crystallization; 2 – front end of crystallization; 3 – pourability limit

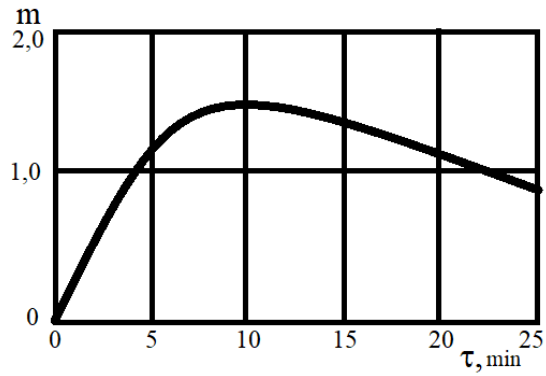


Figure 4. Influence of time on the ratio of solidification rates from above and from the side for cylindrical castings from eutectic gray cast ironм

The finding of the coefficient *m* makes it possible to finally formulate the condition for the beginning of the formation of a concentrated shrinkage shell in cylindrical castings with an open profit part (end). Substituting the values of W_h and W_l into the original equation (29), we obtain the following expression:

$$\frac{m}{\sqrt{B^2+4AFo}}=\frac{\alpha_\upsilon}{\sqrt{B^2+4AFo}}\left\{\frac{3+m_{sr}}{1\text{-}2\alpha_\upsilon}+2\left[\frac{H}{R}+\frac{\alpha_\upsilon\left(3+m_{sr}\right)}{2\alpha_\upsilon-1}-1\right]\times\right.$$

$$\left.\times\left(1+\frac{B}{2A}-\frac{1}{2A}\sqrt{B^2+4AFo}\right)^{2\alpha_\upsilon-1}\right\}. \qquad (45)$$

For castings with an open upper end, the average ratio of solidification rates in the upper and lateral directions is determined by the duration of the crystallization process, that is, by the geometric dimensions of the casting. However, since the rate of lowering of the level of liquid metal for castings with a specific size ratio, for example, $H/R>2$ depends slightly on the value of m_{sr}, in engineering calculations it is permissible to use a constant value of this parameter. In the subsequent calculations, the value is taken for cast iron castings m_{sr}=1,3.

For castings with an open upper end, the average ratio of solidification rates in the upper and lateral directions is determined by the duration of the crystallization process, that is, by the geometric dimensions of the casting. However, since the rate of lowering of the level of liquid metal for castings with a specific size ratio, for example, $H/R > 2$ is weakly dependent on the value of m_{sr}, it is permissible to use a constant value of this parameter in engineering calculations. In the subsequent calculations, the value is taken for cast iron castings $m_{sr} = 1,3$ [9; 10].

Taking into account this assumption, equation (45) takes the following form:

$$\frac{m}{\sqrt{B^2 + 4AFo}} = \frac{\alpha_\upsilon}{\sqrt{B^2 + 4AFo}} \left\{ \frac{4,3}{1\text{-}2\alpha_\upsilon} + 2\left[\frac{H}{R} + \frac{4,3\alpha_\upsilon}{2\alpha_\upsilon - 1} - 1 \right] \times \right.$$

$$\left. \times \left(1 + \frac{B}{2A} - \frac{1}{2A}\sqrt{B^2 + 4AFo} \right)^{2\alpha_\upsilon - 1} \right\}$$

or after reduction

$$m = \alpha_\upsilon \left[\frac{4,3}{1\text{-}2\alpha_\upsilon} 2\left(\frac{H}{R} + \frac{4,3\alpha_\upsilon}{2\alpha_\upsilon - 1} - 1 \right) \left(1 + \frac{B}{2A} - \frac{1}{2A}\sqrt{B^2 + 4AFo} \right)^{2\alpha_\upsilon - 1} \right]. \quad (46)$$

Equations (28) and (46) are solved graphically with respect to the Fourier criterion. To implement this approach, it is necessary to pre-calculate the values of the coefficients *A, B, D, E*. The determination of the specified parameters for iron castings is significantly simplified if the Biot criterion and the relative heat of crystallization L are known.

Let's start with the calculation of the Biot criterion, the change of which over time is described by the following equation:

$$Bi = \frac{b_f R}{\sqrt{\pi}\lambda_m \sqrt{\tau}}, \quad (47)$$

where b_f is the coefficient of heat accumulation of the mold.

Graphically, equation (47) is described by a hyperbolic dependence. The value *Bi* decreases intensively from infinity to a certain level, after which its change slows down significantly. In all subsequent calculations, the average value of the Biot criterion is used, determined from the following expression:

$$Bi_{sr} = \frac{\int_0^{\tau_h} \frac{b_f R}{\sqrt{\pi}\lambda_m \sqrt{\tau}} d\tau}{\int_0^{\tau_h} d\tau} = 2\frac{b_f R}{\sqrt{\pi}\lambda_m \sqrt{\tau}}, \quad (48)$$

where τ_h is the time of solidification of the casting.

2. The Method of Determining the Duration of Solidification of a Casting Using the Fourier Criterion and the Formation of a Shrinkage Shell in Cylindrical Castings

The time of solidification of the casting can be determined using the Fourier criterion. If we substitute the average value of bcp into the original formula (48), we finally have:

$$Bi_{sr} = \frac{2\rho\gamma_m}{(t_{cr} - t_{init})\sqrt{\pi}\lambda_m} \cdot \frac{a}{Fo_h}. \quad (49)$$

On the basis of the values of the Fourier criterion at the end of the crystallization of the casting (see Fig. 4) and equation (49), the values of Bi_{sr} for different grades of cast iron were calculated. The results of this calculation are shown below.

The following values of Bi_{sr} for different brands of alloys are obtained:

magnesium cast iron of pre-eutectic and eutectic compositions – Bi_{sr} = 0,1; magnesium cast iron of the eutectic composition – Bi_{sr} = 0,098; cast iron series of eutectic composition – Bi_{sr} = 0,095.

Calculations were performed at the following values of physical constants: density $\rho = 118,3$ kJ/kg; thermal conductivity coefficient a = 0,025 m^2/hour; coefficient of thermal conductivity of the liquid phase λ_l = 134 kJ/m.h degrees.

Since the values of Bi_{sr} for castings from different grades of cast iron differ slightly, in the subsequent calculations for all cast iron castings we accept the average Bio criterion as equal to Bi_{sr} = 0,1. Next, we determine the value of the dimensionless heat of crystallization. At the same time, we assume that the crystallization temperature interval is Bi_{sr}=0,1, and $t_{cr} = (t_{liq} + t_{solid})/2$ [11]. The temperature of the surface of the mold during the solidification period of cast iron castings according to data [12] is taken equal to $t_{p.f}$ = 900 °C.

Taking this into account, we get:

$$L = \frac{\rho + C_1 \Delta t_{cr}}{\left(C_1 + \frac{\rho}{\Delta t_{cr}} \right)\left(t_{cr} - t_{p.f.} \right)} = \frac{91,0}{0,65 \cdot 306} = 0,46 . \quad (50)$$

The calculation was performed with the following parameter values: $\rho = 268$ kJ/kg; specific heat capacity C_1= 0.753 kJ/kg. degree. The found value of the relative heat of crystallization can only be used to calculate the coefficients *D* and *E*. This parameter is not applicable for determining the coefficients *A* and *B*, since the term containing the variable d_3 was not taken into account in the original equation (16). As a result, the estimated duration of solidification of the casting, obtained according to the specified dependence, will be somewhat overestimated relative to the actual value.

The resulting calculation error can be compensated by an artificial underestimation of *L*. For this purpose, from equation (17) under the condition, for example, $\delta = 1$ we obtain the following expression:

$$A + B = Fo_h . \quad (51)$$

Based on the experimental data shown in Fig. 4, the value of the Fourier criterion is selected at the moment of completion of solidification. Then, the values *A* and *B* are determined from equations (15) and (17), after which expression (50) is solved with respect to the coefficient *L*.

Substitution of the value, for example, $Fo = 2,7$ corresponding to the completion of solidification of castings from pre-eutectic and eutectic magnesium cast irons (see Fig. 5), allows us to obtain the value of the relative heat of crystallization *L* = 0.36. Since the duration of solidification of geometrically identical castings from different grades of cast iron differs slightly, the found value of *L* can be applied to other cast iron alloys with sufficient accuracy for engineering calculations.

Based on the systems of equations (15), (17), (24) and (25), the values of the calculation coefficients are determined: *A, B, D, E.* For cast iron olives, they are *A* = -1.3; *B* = 4.0; *D* = 0.65; *E* = 3.30.

The use of the found coefficients makes it possible to graphically solve equation (28) for castings with a closed profitable part (end). The results of this solution for castings with different geometric ratios for example H/R, volume shrinkage coefficients (α_υ) are presented in fig. 6, a, b. At the points of intersection of the curve of the solidification rate of the casting in

the upper direction W_{cv} with the curves of the change in the rate of fall of the melt level, condition (22) is fulfilled. This moment corresponds to the beginning of the formation of a concentrated shrinking shell, the transverse dimensions of the upper base of which are determined by the spatial position of the boundary of pouring [13; 14]. Based on the systems of equations (15), (17), (24) and (25), the values of the calculation coefficients are determined: *A, B, D, E.* For cast iron olives, they are A = -1.3; B = 4.0; D = 0.65; E = 3.30.

The use of the found coefficients makes it possible to graphically solve equation (28) for castings with a closed profitable part (end). The results of this solution for castings with different geometric ratios for example H/R, volume shrinkage coefficients (α_{υ}) are presented in fig. 6, a, b. At the points of intersection of the curve of the solidification rate of the casting in the upper direction W_{cv} with the curves of the change in the rate of fall of the melt level, condition (22) is fulfilled. This moment corresponds to the beginning of the formation of a concentrated shrinking shell, the transverse dimensions of the upper base of which are determined by the spatial position of the boundary of pouring [13; 14].

With an increase in the parameter, α_{υ} for example, and the geometric ratio, for example, *H/D*, the time required to equalize the rates of lowering of the melt level and solidification of the casting from above is reduced. As a result, a shrinking shell with large dimensions of the upper base is formed. At the same time, shrinkage defects are manifested in the form of porosity in the upper layer of the metal, the intensity of which increases as it approaches the central axis of the casting.

The described character of defect formation is recorded in castings with a ratio for example, $H/D > 4$. In castings with a ratio for example, $H/D < 2$, a similar character of shrinkage is possible only for alloys with a small volume shrinkage coefficient or those with a wide temperature range of crystallization.

If from the moment of the beginning of crystallization, the rate of lowering of the melt level exceeds the rate of solidification of the casting in the upper direction, an open shrinkage shell is formed. At the same time, the dimensions of the upper base of the sink correspond to the dimensions of the upper end of the casting. Due to the intense drop in the level of the liquid phase, the hard metal crust formed during upper cooling either has

minimal thickness and strength, or fails to form. This leads to its continuous displacement following the melt mirror until the solidification of the casting is complete [13; 14].

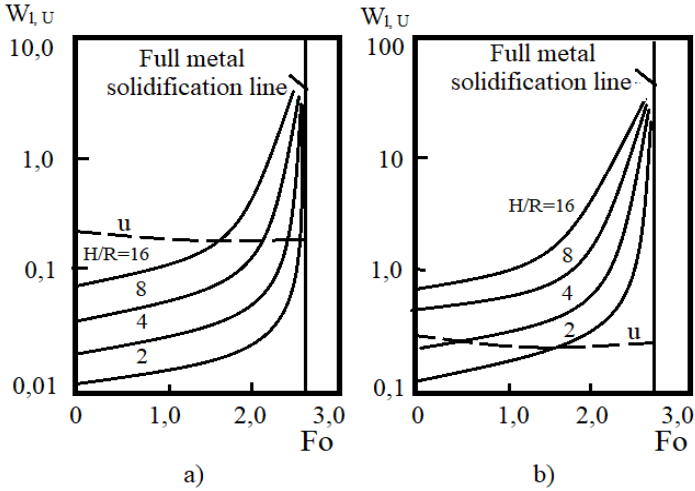


Figure 5. Dependence of the dimensionless velocities of the melt level lowering W_l and solidification of the casting from above W_{cv} on the Fourier criterion for castings with a closed top: a – at α_v = 0,01; b – at α_v = 0,08

In intermediate cases, a concentrated shrinkage shell is formed under the layer of the porous upper crust of the metal.

The geometrical parameters of the upper base of the shrinking shell depend on the spatial position of the pourability boundary at the time of the defect's origin. This time point is fixed by the intersection of the kinetic curves of the rate of fall of the melt level and the rate of solidification of the casting from above. The coordinate of the pourability boundary for this moment of time is found by the experimental curves of the solidification kinetics (see Fig. 5). Therefore,

$$r = R - R\delta' = R\left(1 - \delta'\right), \qquad (51)$$

where r – radius of the contour of the upper base of the shrink shell;

δ' – the relative coordinate of the flow boundary at the time of the onset of the shrinking shell.

The thickness of the upper shrink crust for castings with a closed top is determined by the expression:

$$h_m = R\delta'. \quad (52)$$

Assuming that the concentrated shrinkage shell has the form of a straight truncated cone (where the upper diameter is found according to equation (51), and the lower diameter is equal to the distance between the pourability and feeding boundaries at the moment when the pourability front reaches the axis of the casting), its depth can be determined according to the calculation scheme in Fig. 6.

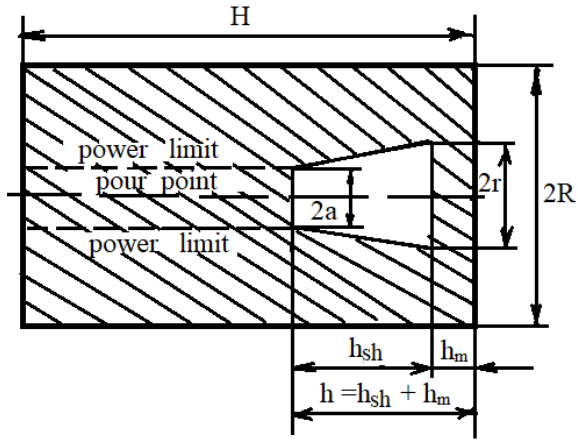


Figure 6. Calculation scheme for the formation of a concentrated shrinkage shell in cylindrical castings with a closed end

$$h_{sh} = \frac{\alpha_\upsilon V}{S} = \frac{3\alpha_\upsilon H}{(1-\delta')(1-\delta'+n)+n^2}, \quad (53)$$

where $V = \pi R^2 H$ – is the volume of the cylindrical casting;

$S = \frac{\pi R^2}{3} = \left[(1-\delta')(1-\delta'-n)+n^2\right]$ – the average cross-sectional area of the concentrated shrink shell;

$n = a/R -$ parameter of the shape of the shrinkage defect:

a – the width of the liquid-solid zone at the moment the casting front reaches the central axis of the casting.

The depth of the spread of shrinkage defects in the casting is determined based on the geometric characteristics of the shell cone and the thickness of the bridges.

$$h = h_{sh} + h_m = \frac{3\alpha_\upsilon H}{(1-\delta')(1-\delta'+n)+n^2} + R\delta' . \quad (54)$$

The results of the graphical solution of equation (46) for castings with an open upper surface are shown. Analysis of these dependences, obtained for castings with a radius of R = 2 cm and 8 cm, shows that the curves of the metal solidification rate from above are generally located higher compared to castings with a closed upper part. At the same time, they intersect twice with the curves of the rate of decrease in the level of the liquid phase.

Due to the low relative solidification rate of the casting from above at the initial stage of crystallization, the concentrated shrinkage cavity is initially formed as open, and the diameter of its base coincides with the diameter of the upper part of the casting. However, the intensive growth of the crystallization rate of the upper zone leads to the fact that it exceeds the rate of decrease in the level of the liquid phase. At this moment, the development of the concentrated shrinkage cavity stops. A crystallized bridge is formed, the thickness of which increases until the rate of lowering the metal mirror again exceeds the rate of solidification from above. In the future, the concentrated shrinkage cavity continues to develop until the casting limit reaches the axis of the casting. The nature of the location of shrinkage defects for this case is schematically shown in Fig. 7. An experimental study of the distribution of shrinkage cavities in cylindrical castings with an open top made of magnesium cast iron in wet sand-clay molds confirmed a high degree of coincidence of the theoretical model with experimental data [15; 16].

The nature and spatial distribution of shrinkage cavities can vary depending on the material, geometric parameters of the casting and technological conditions of its pouring. In particular, in the absence of a second intersection point of the velocity curves, the lower part of the shrinkage cavity is not formed due to the formation of a porous bridge of considerable thickness. In addition, in the case of metal supply from

below (siphon pouring), there is a possibility that the upper layer of the melt will begin to crystallize more intensively than the rest of the casting volume. Under such conditions, the upper part of the shrinkage cavity is not formed, and its configuration becomes similar to castings with a closed upper surface (Fig. 7).

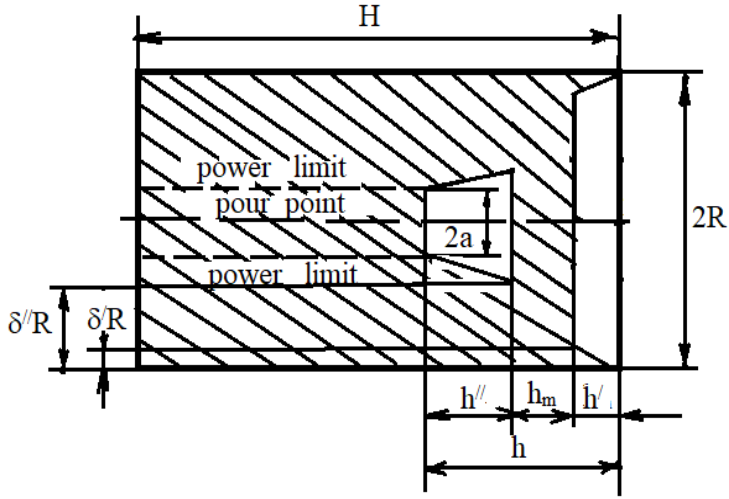


Figure 7. Scheme of the formation of a shrinking shell in cylindrical castings with an open top

The calculation of the depth of shrinkage defects in castings with an open upper surface is performed according to the following dependence:

$$h = h' + h_{\text{m}} + h'', \tag{55}$$

where h' is the depth of the upper open zone of the shrinkage cavity;

h_{m} – the thickness of the crystal bridges;

h'' – the depth of the closed zone of the shrinkage cavity.

The value of the bridge thickness can be calculated using the following relationship:

$$h_{\text{m}} = m''_{\text{sr}} R\left(\delta'' - \delta'\right), \tag{56}$$

where δ'' – is the relative coordinate of the pourability limit at the moment of the second effective value of the metal lowering and solidification rates from above;

m_{sr} – the average ratio of the casting crystallization rates in the upper and lateral zones for the time interval from the beginning of solidification to the moment when the metal level reduction rate is equal to the solidification rate from above for the second time.

The value of the tsr coefficient can be approximately found from the expression:

$$m''_{sr} = \frac{m''}{2}, \tag{57}$$

where m'' – is the ratio of the crystallization rates of the casting from the top and the side at the moment of the second equalization of the rate of metal level decrease and the rate of its solidification from the top.

The volume of the upper part of the shrinkage shell is determined by the shrinkage of the metal that solidified until the moment when the rate of crystallization from the top became greater than the rate of lowering of the liquid metal. At this moment, the thickness of the crystallized layer from the side and bottom of the casting is $R\delta'$. The volume of the specified metal zone can be found using geometric calculations [16; 17].

$$V' = \pi R^2 \left[\delta' R \left(1-\delta'\right)^2 + 2\left(1-\frac{\delta'}{2}\right) H\delta' \right]. \tag{58}$$

Under these conditions, the depth of the upper open zone of the shrinkage cavity can be calculated using the following formula:

$$h' = \frac{\alpha_{\upsilon} \dot{V}'}{S'}, \tag{59}$$

where S' – is the average cross-sectional area of this shrinkage cavity zone

$$h' = \frac{3\alpha_{\upsilon} \left[\delta' R \left(1-\delta'\right)^2 + 2\left(1-\frac{\delta'}{2}\right) H\delta' \right]}{3-3\delta'+\delta'^2}. \tag{60}$$

The value h'' is determined similarly, taking into account that by the time the closed part of the shrinkage cavity is formed, a volume of metal equal to has already solidified h''.

Then.

The value of the parameter h'' is determined similarly, taking into account that by the time the closed part of the shrinkage cavity is formed, a volume of metal equal to has already crystallized V'.

Under the following conditions:

$$h'' = \frac{\alpha_{\upsilon}\left(V - V'\right)}{S''} = \frac{3\alpha_{\upsilon}\left[H - R\left(1-\delta'\right)^2\delta' - 2H\left(1-\frac{\delta'}{2}\right)\delta'\right]}{\left(1-\frac{\delta''-\delta'}{1-\delta'}\right)\left(1-\frac{\delta''-\delta'}{1-\delta'}+n\right)+n^2}. \quad (61)$$

After substituting expressions (56), (60) and (61) into equation (55), we obtain a dependence for determining the depth of propagation of shrinkage defects in castings with an open upper surface.

$$h = \frac{3\alpha_{\upsilon}\left[\delta R\left(1-\delta'\right)^2 + 2\left(1-\frac{\delta'}{2}\right)H\delta'\right]}{3-3\delta'+\delta'^2} + \frac{3\alpha_{\upsilon}\left[H - R\left(1-\delta'\right)^2\delta' - 2H\left(1-\frac{\delta'}{2}\right)\delta'\right]}{\left(1-\frac{\delta''-\delta'}{1-\delta'}\right)\left(1-\frac{\delta''-\delta'}{1-\delta'}+n\right)+n^2} + m''_{sr}R\left(\delta''-\delta'\right). \quad (62)$$

Practical application of the calculated dependencies (54) and (62) requires preliminary determination of the shape coefficient n. For this purpose, a series of experimental castings in wet sand-clay molds was carried out. Experimental cylindrical castings were made with an open and closed top. The geometric parameters of the samples were: diameter 80 and 100 mm at a height of 200 mm, as well as a diameter of 120 mm at a height of 300 mm. Gray cast iron of the SCh 25-30 brand and hypoeutectic cast iron with spheroidal graphite were used for the research. Filling the molds with liquid metal was carried out from below using a siphon supply. Longitudinal templates with a thickness of 15 mm were made from all the obtained castings. The shape coefficient n was determined by the results of direct measurement of the lower base of the cone of the shrinkage cavity on these samples. The average value of the coefficient n for castings from hypoeutectic magnesium cast iron was 0.30, while for gray cast iron of the SCh25-30 brand this indicator was 0.26 [17; 18].

Based on the calculated dependencies (54) and (56), the established value of the coefficient *n*, data on the hardening kinetics of cylindrical castings

(Fig. 5), as well as the value α_{υ} for hypoeutectic magnesium cast iron, the depth of shrinkage defects in a series of real castings was calculated. The results of the theoretical calculation and experimental data in all cases demonstrated a high degree of convergence, which confirms the validity of the initial theoretical provisions of the proposed method. The practical application of this technique, in the presence of data on crystallization kinetics, allows predicting the spatial location of shrinkage cavities in castings of arbitrary configuration made from base casting alloys [19; 20].

CONCLUSIONS

Analysis of the data allows us to state: the nature of the migration of solid and liquid phases during solidification of cast iron directly depends on the degree of malleability of the casting mold. If the design of the mold prevents pre-shrinkage expansion, the excess metal does not increase the external dimensions of the product, but moves inward, filling the resulting shrinkage shell.

It is possible to visualize the described processes by clearly demonstrating how cast iron castings behave during solidification in the conditions of malleable and hard (non-malleable) forms.

At the first stage (immediately after pouring), metallostatic pressure acts on the malleable form, causing its expansion. As a result, the volume of the cavity increases, and the metal level drops. This decline, together with the shrinkage of the melt, is compensated by the additional flow of liquid metal from the sprue system. In a hard (inflexible) form, the volume of the structure does not change, so the decrease in the metal level is caused exclusively by its shrinkage in the liquid state.

At the initial stage of hardening and formation of the shrink shell (II stage), the surface of the casting is covered with a thin hard layer, which at first has low strength. Since the casting form is malleable, under the influence of the internal pressure of the liquid metal, this crust is deformed, which leads to further expansion of the casting. In addition, the volume of the product may increase due to the linear expansion of the outer layer caused by the graphitization process. The decrease in volume and shrinkage of the liquid alloy lead to a drop in its level, which at this stage can be compensated exclusively by the separation of the graphite phase. Such a process is possible only in pre-eutectic cast irons, since the supply of melt

from the sprue system at this point already stops or becomes insignificant.

Due to the rigidity of the form, the volume of the casting cannot increase, which slows down the process of the melt level falling inside the hardening outer crust.

The use of forms with intensive heat dissipation (for example, on the basis of quick-drying mixtures) accelerates the solidification of a strong surface layer, which restrains the internal pressure of the liquid metal and prevents the expansion of the casting.

At the final stage (stage III), cast iron crystallizes over the entire volume of the workpiece, which is accompanied by the growth of shrinkage defects. Since the casting mold is malleable, graphitization causes volume expansion of the alloy in all directions. At the same time, the displacement of the metal to the periphery and along the borders of the form increases the dimensions of the casting, which entails the growth of internal voids. On the contrary, the inflow of melt directed inside the part contributes to the reduction of the volume of the shrinkage shells.

In such conditions, only an insignificant share of volume expansion is spent on compensation of shrinkage defects. When using rigid, non-deformable casting forms, this expansion is completely redistributed into the inner layers, contributing to the elimination of the formed shrinkage voids. As a rule, this ensures the complete elimination of defects and can lead to the displacement of excess alloy on the surface, which is typical for casting in a metal mold. Changing the geometry of the casting directly affects the capacity of the shrink shells, and the directed movement of the melt inside the casting body minimizes the total volume of defects.

References:

1. Bialyk A.H., Naumyk V. V., Lunov A.V. (2013). *Teoriia lyvarnykh splaviv: navchalnyi posibnyk* [Theory of Foundry Alloys: тextbook]. Zaporizhzhia. ZNTU. 156 p. (in Ukrainian)

2. Leibenzon V.O., Piliushenko V.L., Kondratenko V.M., Khrychykov V.Ie. (2009). *Tverdnennia metaliv i metalevykh kompozytsii: pidruchnyk* [Hardening of metals and metal compositions: textbook]. Kyiv: Naukovovyrobnyche pidpryiemstvo «Vydavnytstvo «Naukova dumka» NAN Ukrainy, 447 p. (in Ukrainian)

3. Verkhovliuk A. M., Narivskyi A. V., Mohylatenko V. H. (2016). *Tekhnolohii oderzhannia metaliv ta splaviv dlia lyvarnoho vyrobnytstva: navchalnyi posibnyk*:

[Technologies for producing metals and alloys for foundry production: a training manual]. In Naydek V.L. (Ed). Kyiv: Vinichenko, 223 p. (in Ukrainian)

4. Bialik H. A., Naumyk V. V., Tsyvirko E. I. (2013). *Praktykum z teorii lyvarnykh splaviv ta protsesiv: navchalnyi posibnyk* [Workshop on the theory of casting alloys and processes: a textbook]. Zaporizhzhia: ZNTU, 98 p. (in Ukrainian)

5. Mohylatenko V. H. (2011). *Teoretychni osnovy lyvarnoho vyrobnytstva: navchalnyi posibnyk* [Theoretical foundations of foundry production: a textbook]. Natsionalnyi tekhnichnyi universytet "Kharkivskyi politekhnichnyi instytut". Kharkiv. NTU "KhPI", 287 p. (in Ukrainian)

6. Lysenko T. V. (2014). Teoretychni *osnovy formuvannia vylyvkiv: navchalnyi posibnyk* [Theoretical foundations of casting formation: a textbook]. Natsionalnyi tekhnichnyi universytet "Kharkivskyi politekhnichnyi instytut". Kharkiv. NTU "KhPI", 191 p. (in Ukrainian)

7. Lysenkov V. Yu. (2025). Modeliuvannia formuvannia usadkovykh rakovyn u stalnykh vylyvkakh typu "Korpus" [Modeling the formation of shrinkage cavities in steel castings of the "Body" type]. Informatsiini tekhnolohii: nauka, tekhnika, tekhnolohiia, osvita, zdorovia: materialy 33-yi Mizhnarodnoi naukovo-praktychnoi konferentsii (m. Kharkiv 14-17 travnia 2025). Natsionalnyi tekhnichnyi universytet" Kharkivskyi politekhnichnyi instytut". Kharkiv: NTU "KhPI", 394 p.(in Ukrainian)

8. Pienziev P. S., Frolova L. V., Lysenkov V. Yu., Lavryk Ye. Ye. (2024). Vplyv konstruktsii nadlyshkiv na formuvannia usadkovykh rakovyn u stalevykh vylyvkakh pry lytti v razovi pishchani formy [The influence of the design of surpluses on the formation of shrinkage cavities in steel castings when casting in disposable sand molds]. *Industrial and technology systems*. Vol. 4, №1(78), pp. 6-10. DOI: https://doi.org/10.15587/2706-5448.2024.310424 (in Ukrainian)

9. Lu S., Lu D., Li Y., & Chen Y. (2026). Multi-Objective Optimization of Casting Parameters for Mn70Ni25Cr5 Alloy Using ProCAST Simulation and Response Surface Methodology. *Metals*, *16*(7), 813.

10. Kovalova A. V. (2020). *Teoretychni ta praktychni aspekty zhyvlennia vylyvkiv iz vysokomitsnoho chavunu z kuliastym hrafitom (VChShH): mahisterska robota* [Theoretical and practical aspects of feeding castings from high-strength cast iron with spheroidal graphite (HSG): master's thesis]. Zaporizhzhia: ZNTU, 98 p. (in Ukrainian)

11. Kotliarskyi F.M. (2020). Isnuiuchi uiavlennia pro vplyv vodniu na vlastyvosti aliuminiievykh splaviv. Povidomlennia 2 [Existing ideas about the influence of hydrogen on the properties of aluminum alloys. Message 2]. *Protsesy lyttia - Casting processes*, vol. 139, no 1, pp. 3-19. DOI: https://doi.org/10.15407/plit2020.01.003 (in Ukrainian)

12. Kropivnyi V. M., Bosyi M. V., Kuzyk O. V.,. Kropivna A. V,. Molokost L. A. (2022). Osoblyvosti formuvannia likvatsii ta yii naslidky u vylyvkakh z vysokomitsnoho chavunu [Features of the formation of liquation and its consequences in high-strength cast iron castings]. Materialoznavstvo ta tekhnolohii: Mizhnarodna naukovo-tekhnichna konferentsiia 22–23 veresnia 2022. Kharkivskyi natsionalnyi avtomobilno-dorozhnii universytet. Kharkiv, pp. 124–129. Available at: https://dspace.khadi.kharkov.ua/handle/123456789/19162 (in Ukrainian)

13. Khrychykov V. Ye., Semenov O. D., Meniailo O. V., Shalevska I. A., Mianovska Ya. V. (2021). Usunennia utiazhyny u khudozhnikh vylyvkakh z riznoiu tovshchynoiu stinky [Elimination of heaviness in artistic castings with different wall thicknesses]. *Protsesy lyttia,* Tom 146 № 4, pp. 14–21. DOI: https://doi.org/10.15407/plit2021.04.014 (in Ukrainian)

14. Penzev P. S., Lavryk Ye. Ye., Lysenkov V. Yu. (2024). Vplyv konstruktsii nadlyshkiv na formuvannia usadkovykh rakovyn u stalevykh vylyvkakh typu "korpus" [The influence of overburden design on the formation of shrinkage cavities in "case" type steel castings]. Nemetalevi vkraplennia i hazy u lyvarnykh splavakh: zbirnyk tez 17-yi Mizhnarodnoi naukovo-tekhnichnoi konferentsii 26-27 lystopada 2024. Natsionalnyi universytet "Zaporizka politekhnika". Zaporizhzhia, pp. 42-44. Available at: https://zp.edu.ua/uploads/dept_s&r/2024/conf/1.5/NMGCA-2024.pdf (in Ukrainian)

15. Yevtushenko N. S., Ponomarenko O. I. (2022). Kompleksnyi pidkhid shchodo zapobihannia defektiv ta bezpeky u lyvarnomu vyrobnytstvi [A comprehensive approach to defect prevention and safety in foundry production]. Materialy XVIII Mizhnarodnoi naukovo-praktychnoi konferentsii «Lytvo. Metalurhiia. 2022». (04–06 zhovtnia 2022). Kharkiv, NTU «KhPI», pp. 61–63. (in Ukrainian)

16. Smirnov, O. M., Verzilov O. P., Ukhin V. Ye., Kulish Yu. Yu., Hoida D. I. (2019). Osoblyvosti formuvannia usadkovoi rakovyny v umovakh rozlyvannia stali na mashynakh napivbezperervnoho lyttia zahotivok [Features of the formation of a shrinkage cavity in the conditions of steel casting on semi-continuous casting machines]. *Protsesy lyttia*. № 6 (138), pp. 30–37. DOI: https://doi.org/10.15407/plit2019.06.030 (in Ukrainian)

17. Bilyi O. P., Solonenko L. I., Osypenko I. O., Usenko R. V., Repiakh S. I., Khrychykov V. Ye. (2021). Doslidzhennia umov utvorennia usadkovoi rakovyny v nyzhnii shyitsi prokatnykh valkiv vykonannia SPKhN-60 [Research into the conditions for the formation of a shrinkage cavity in the lower neck of rolling rolls of the SPKHN-60 design.]. *Teoriia i praktyka metalurhii.* № 6 (131), pp. 39–47. DOI: https://doi.org/10.34185/tpm.6.2021.06. (in Ukrainian)

18. Kunytskyi Yu.A., Tserehradska T.L. (2002). *Termodynamika metaliv i splaviv: navchalnyi posibnyk* [Thermodynamics of Metals and Alloys: A Study Guide.]. Kyiv. Akademperiodyka, 73 p. (in Ukrainian)

19. Bosyi. M.V. (2026). Termodynamika fazovykh perekhodiv i dyfuziinykh protsesiv pry doslidzhenni lyvarnykh vlastyvostei splaviv [Thermodynamics of phase transitions and diffusion processes in the study of the casting properties of alloys]. *Multidisciplinární mezinárodní vědecký magazín Věda a perspektivy*. № 3(58), pp. 223-241. DOI: https://doi.org/10.52058/2695-1592-2026-3(58)-223-241(in Ukrainian)

20. Kropivnyi V.M., Bosyi M.V., Kuzyk O.V., Kropivna A.V., Molokost L.A. (2024). Termodynamichni zakonomirnosti strukturoutvorennia vysokomitsnoho chavunu pry modyfikuvanni ta riznykh umovakh krystalizatsii rozplavu [Thermodynamic principles of structure formation in high-strength cast iron during inoculation and under various melt crystallization conditions]. *Tsentralnoukrainskyi naukovyi visnyk. Tekhnichni nauky.* Vyp. 9(40), ch. I, pp. 27-36. DOI: https://doi.org/10.32515/2664-262X.2024.9(40).1.27-36 (in Ukrainian)